

Dalton Transactions - Full Article

**Transition Metal Complexes of Antimony Centered Ligands based upon Acenaphthyl
Scaffolds. Coordination Non-Innocent or Not?**

Sinas Furan,^a Emanuel Hupf,^a Julian Boidol,^a Julian Brünig,^a Enno Lork,^a

Stefan Mebs,^b* Jens Beckmann^a*

^a *Institut für Anorganische Chemie, Universität Bremen, Leobener Straße 7, 28359 Bremen,
Germany*

^b *Institut für Experimentalphysik, Freie Universität Berlin, Arnimallee 14, 14195 Berlin,
Germany*

Received

Supporting Information

* Correspondence to Jens Beckmann (E-mail: j.beckmann@uni-bremen.de) and Stefan Mebs (E-mail: steb@chemie.fu-berlin.de)

Table of Contents

Figures S1a-c.	NMR spectra of 1
Figures S2a-c.	NMR spectra of 2
Figures S3a-c.	NMR spectra of 3
Figures S4a-c.	NMR spectra of 4
Figures S5a-c.	NMR spectra of 5
Figures S6a-c.	NMR spectra of 6
Figures S6d.	UV/Vis spectrum of 6
Table S1.	Selected interatomic distances (Å) and angles (°) of 1 and 2
Figure S7.	AIM topologies, NCI <i>iso</i> -surfaces and ELI-D <i>iso</i> -surfaces of 1 and 2
Figure S8.	AIM topologies, NCI <i>iso</i> -surfaces and ELI-D <i>iso</i> -surfaces of 5
Figure S9.	AIM topologies, NCI <i>iso</i> -surfaces and ELI-D <i>iso</i> -surfaces of 6

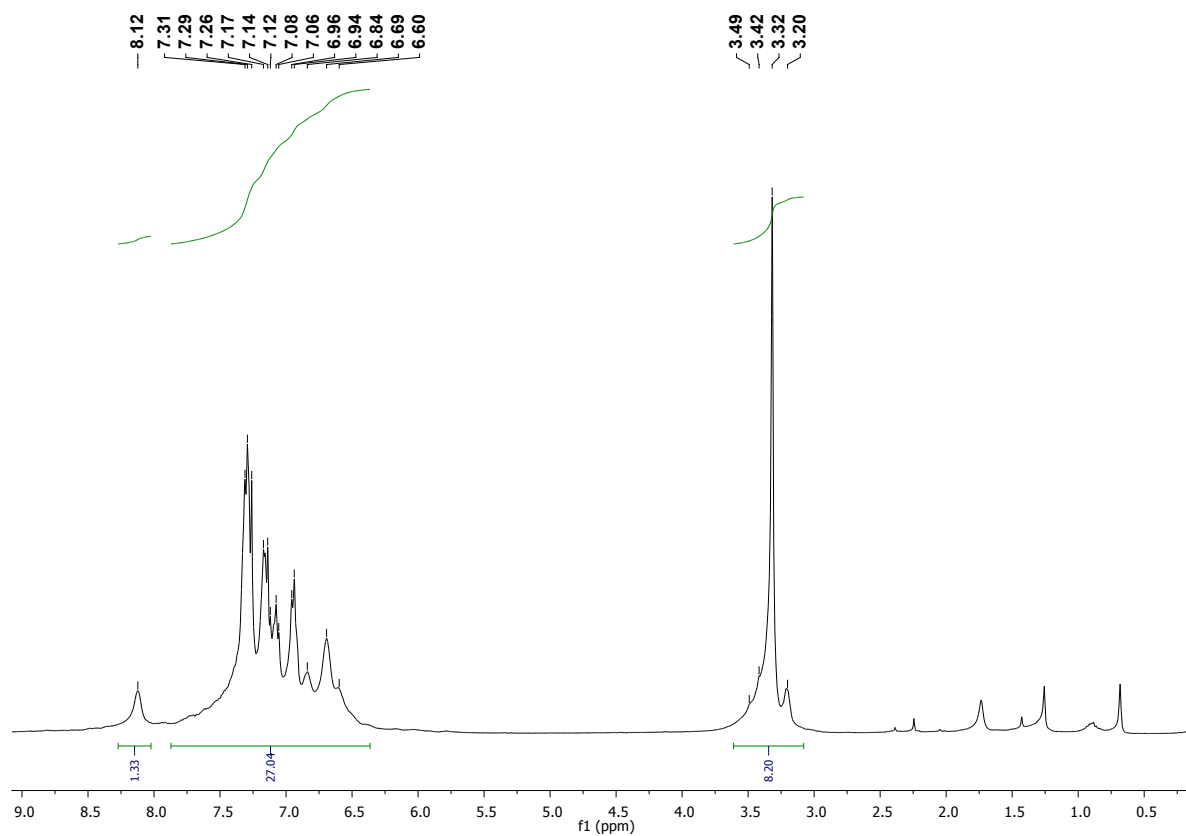


Figure S1a. ^1H -NMR spectrum (CDCl_3) of **1**.

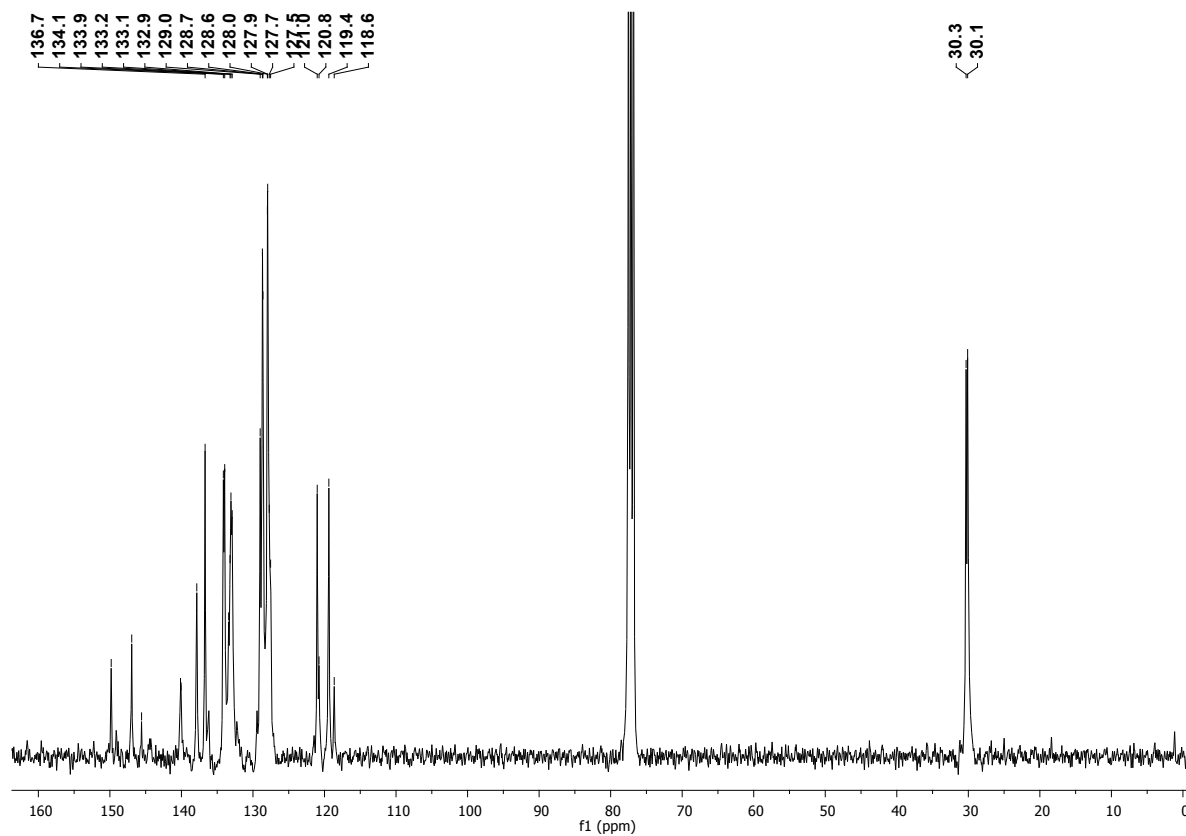


Figure S1b. $^{13}\text{C}\{^1\text{H}\}$ -NMR spectrum (CDCl_3) of **1**.

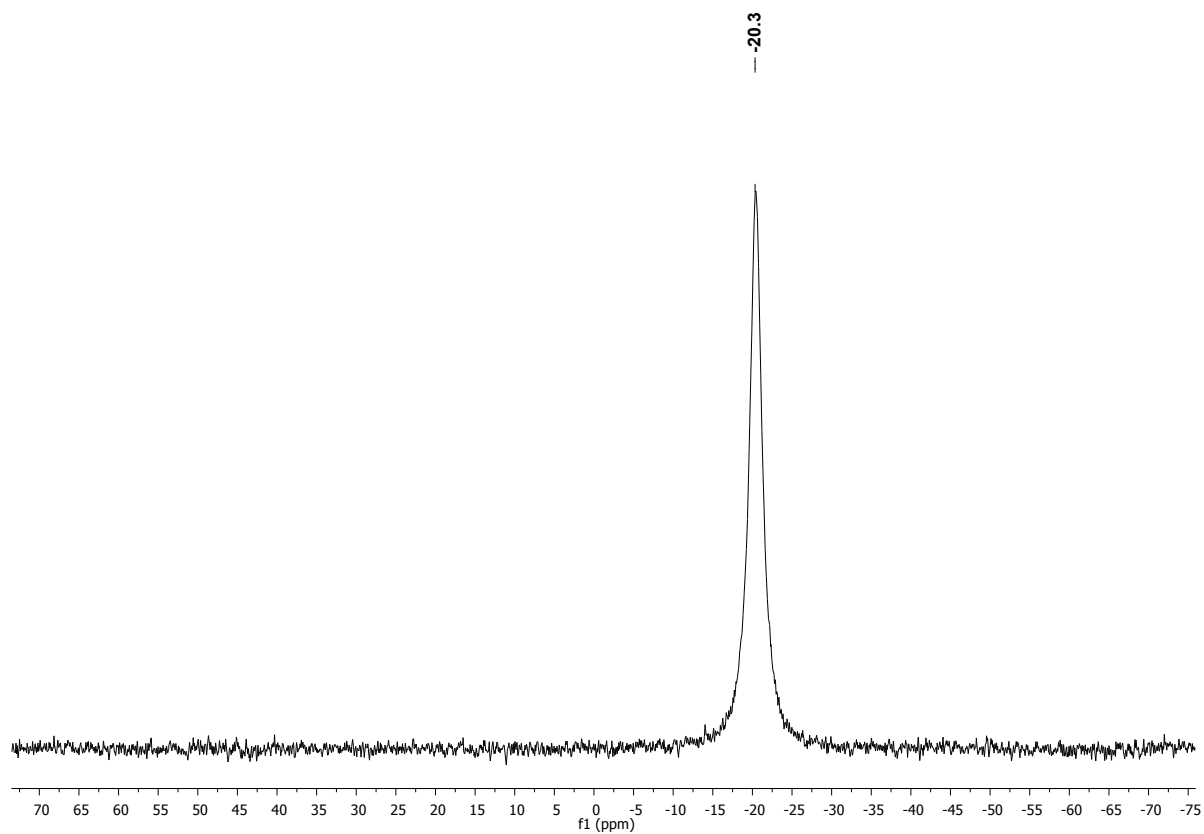


Figure S1c. ³¹P{¹H}-NMR spectrum (CDCl₃) of 1.

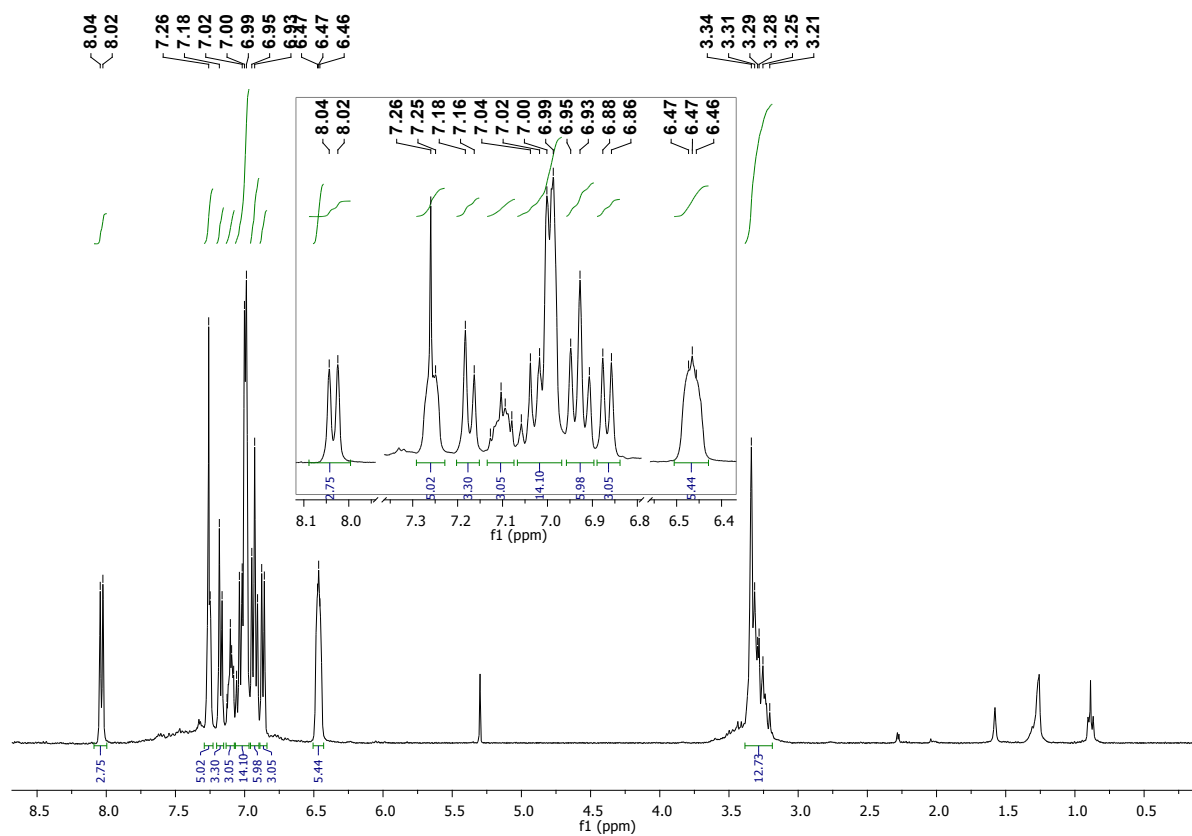


Figure S2a. ¹H-NMR spectrum (CDCl₃) of 2.

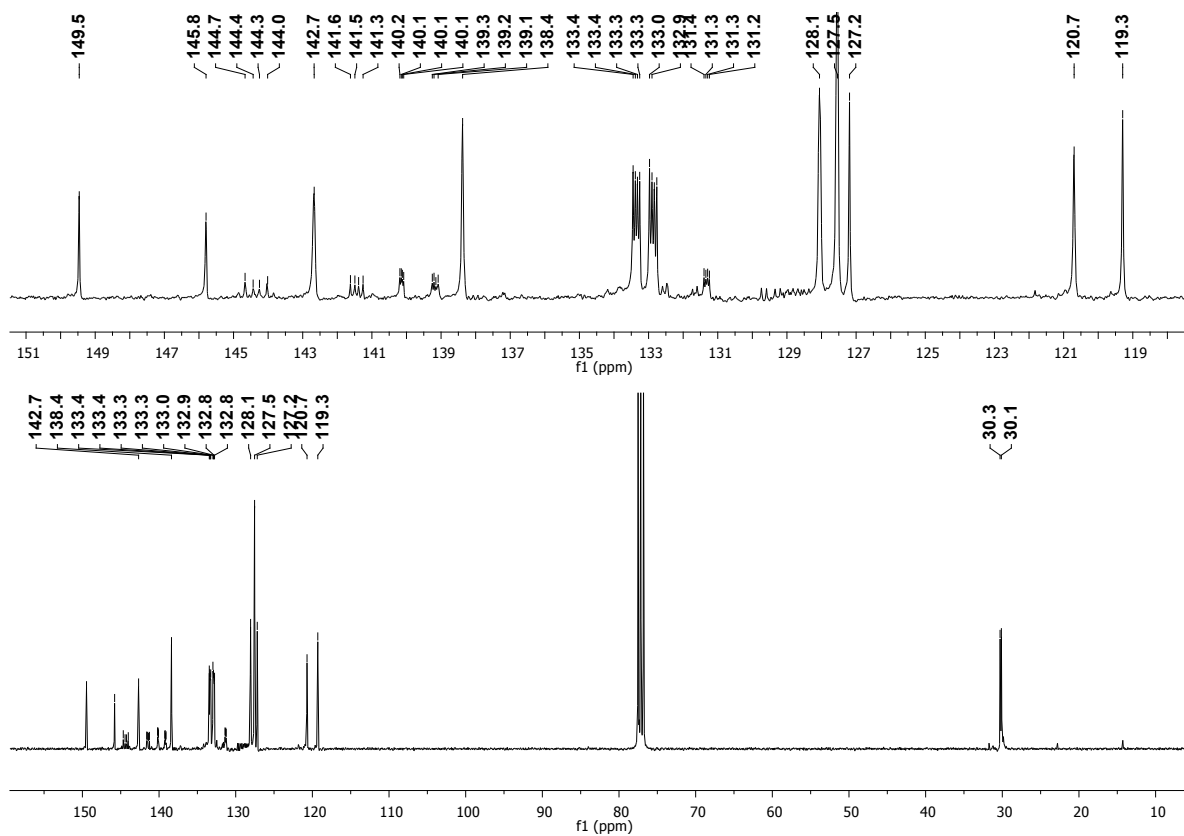


Figure S2b. $^{13}\text{C}\{^1\text{H}\}$ -NMR spectrum (CDCl_3) of **2**.

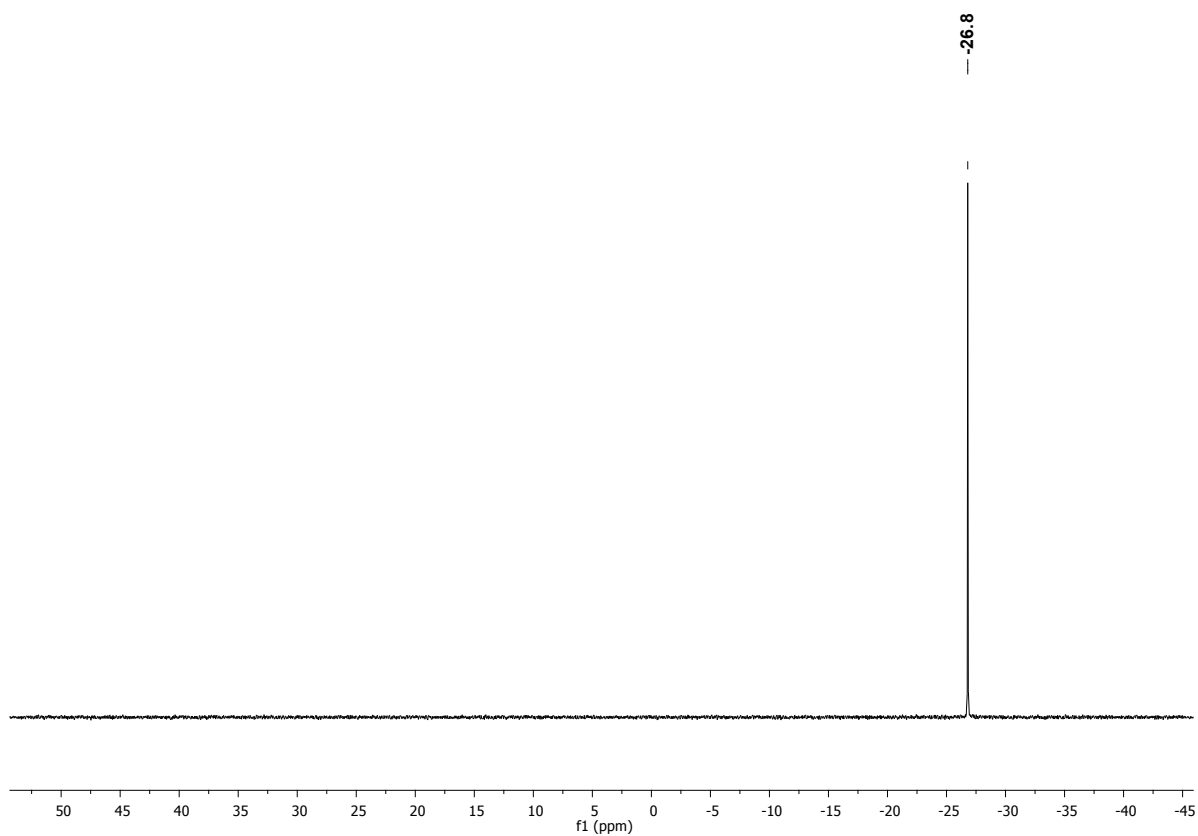


Figure S2c. $^{31}\text{P}\{^1\text{H}\}$ -NMR spectrum (CDCl_3) of **2**.

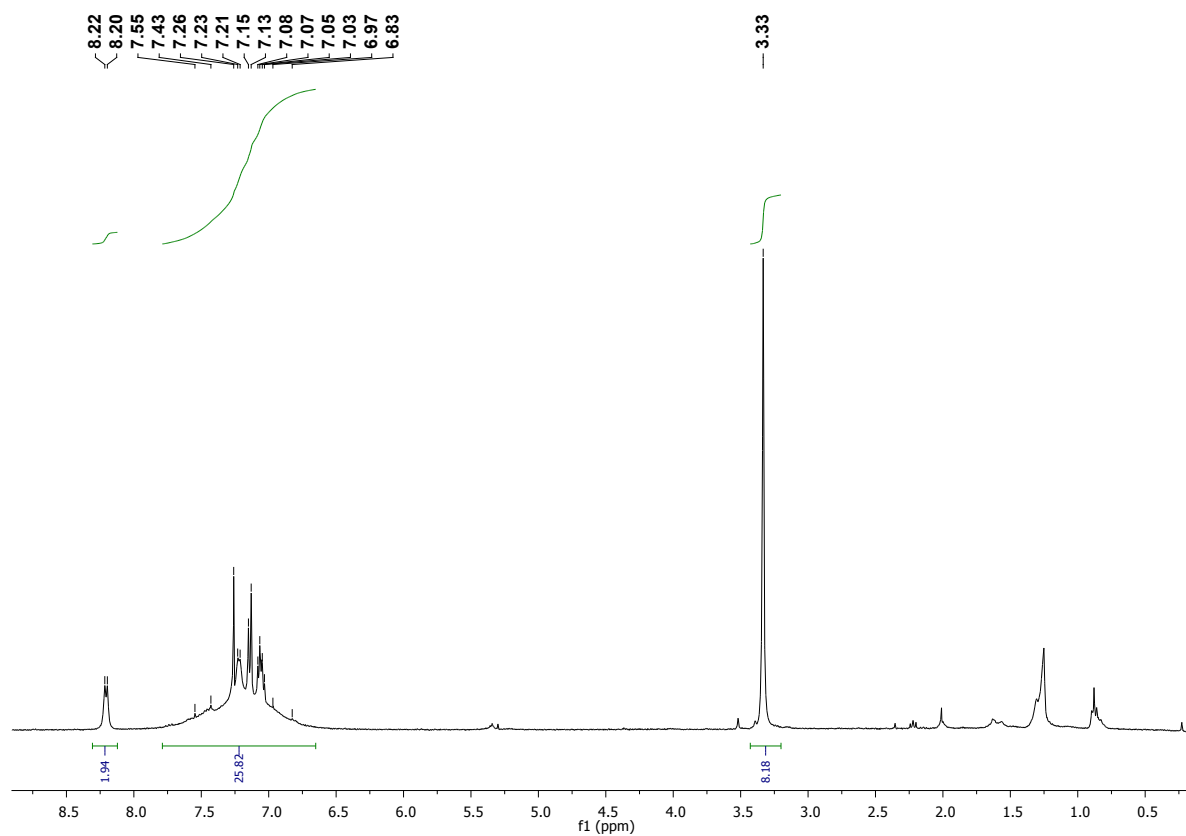


Figure S3a. ^1H -NMR spectrum (CDCl_3) of **3**.

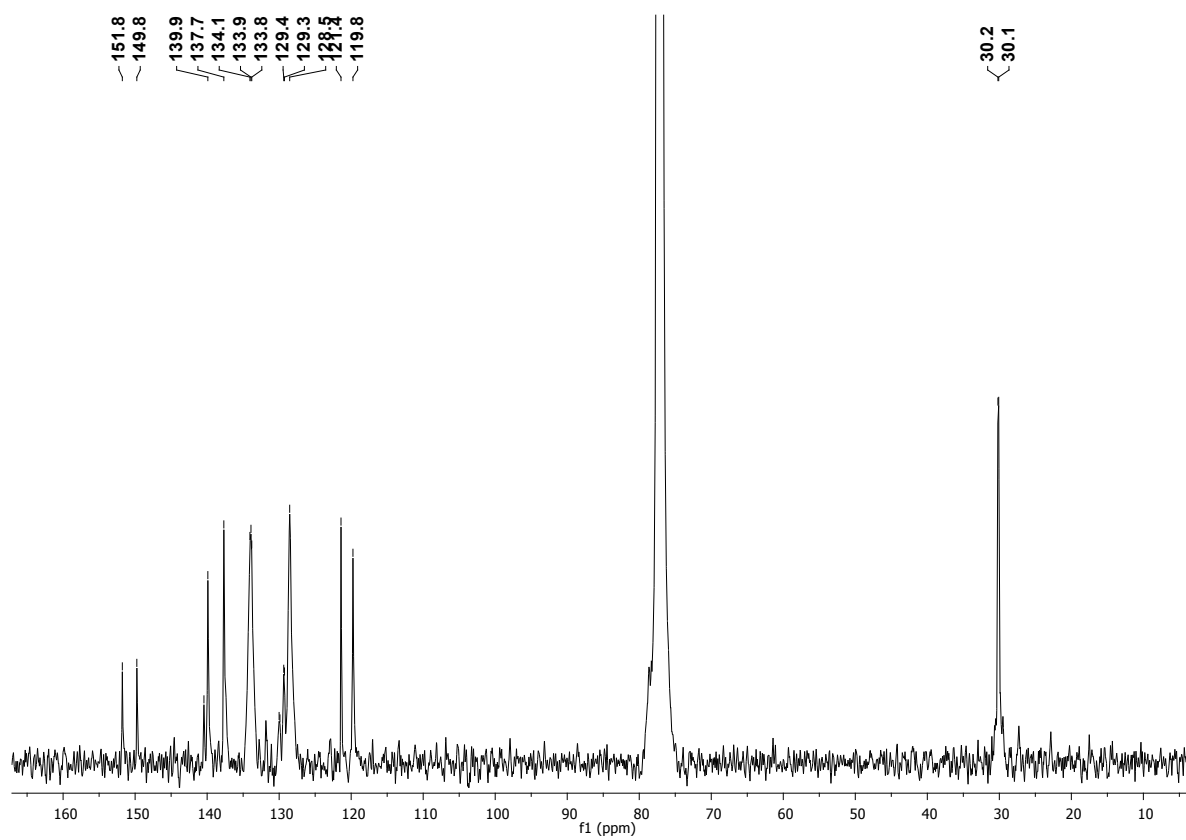


Figure S3b. $^{13}\text{C}\{^1\text{H}\}$ -NMR spectrum (CDCl_3) of **3** (poor solubility, acquisition time 48 h).

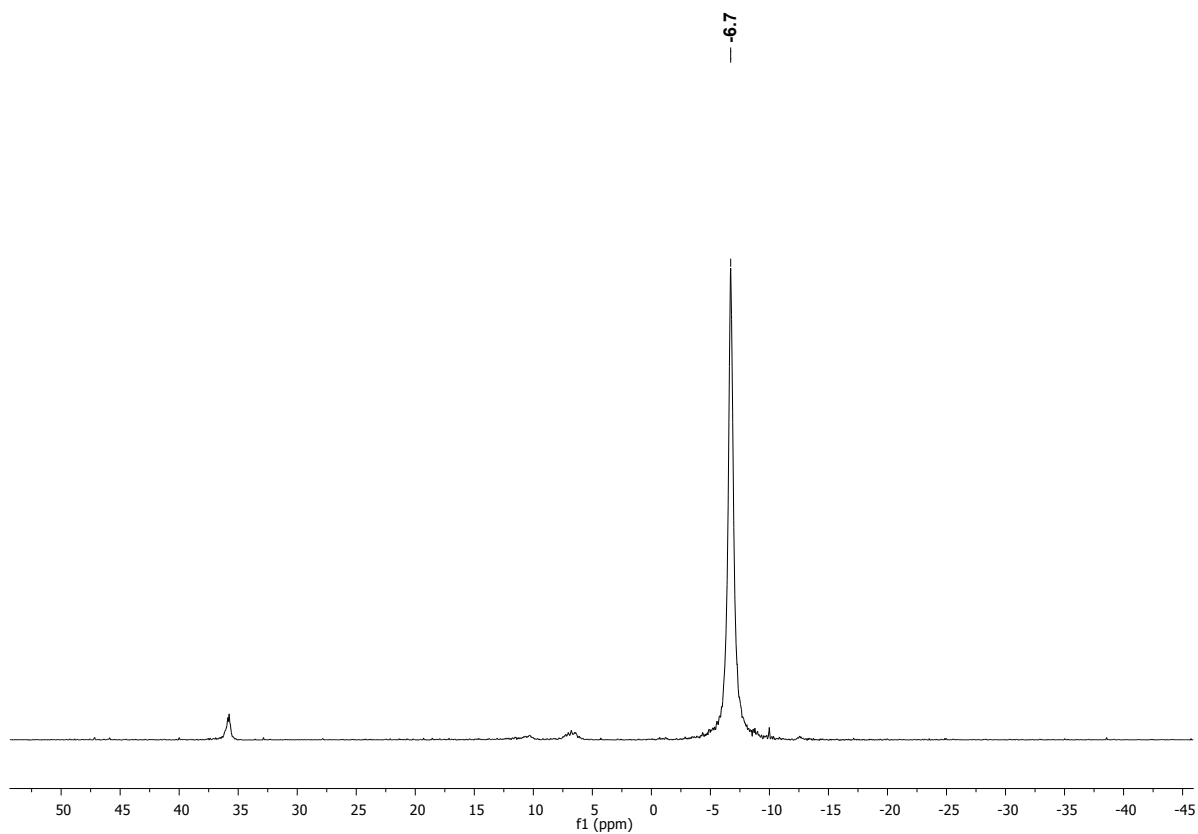


Figure S3b. ³¹P{¹H}-NMR spectrum (CDCl₃) of 3 (poor solubility, acquisition time 12 h).

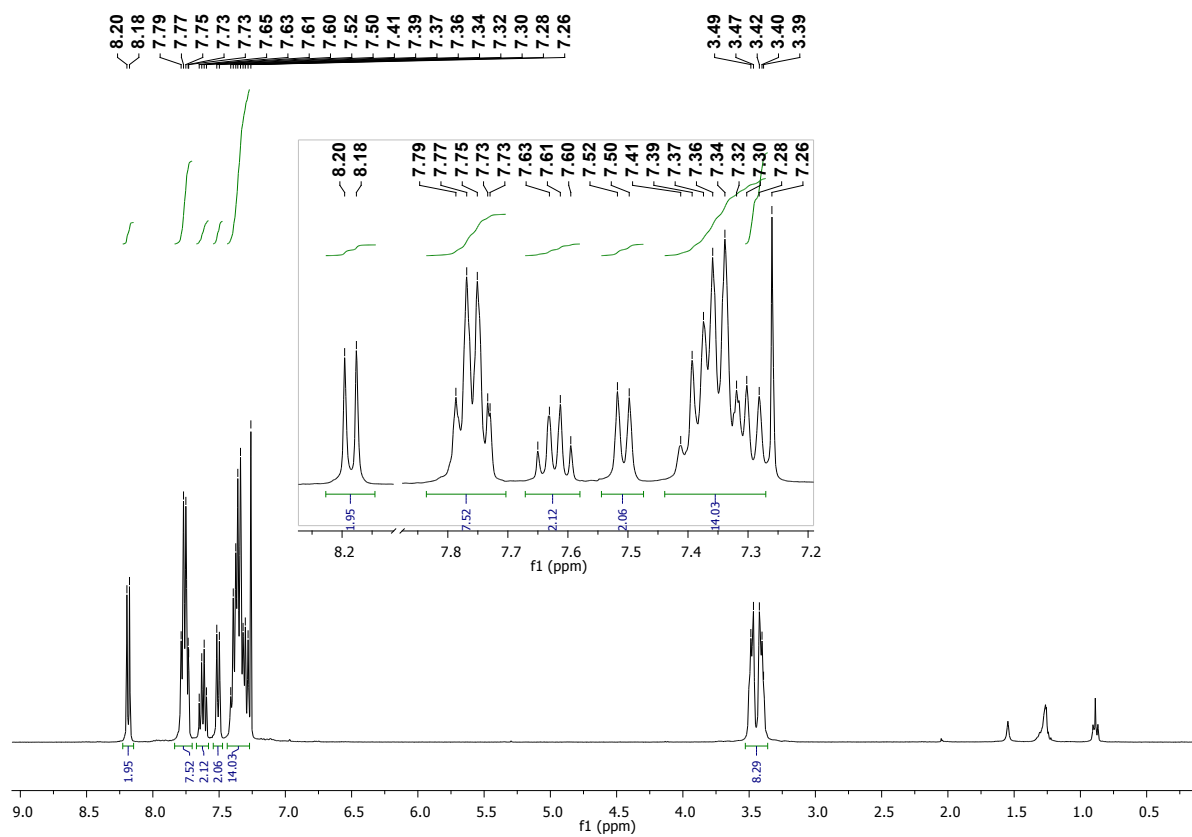


Figure S4a. ¹H-NMR spectrum (CDCl₃) of 4.

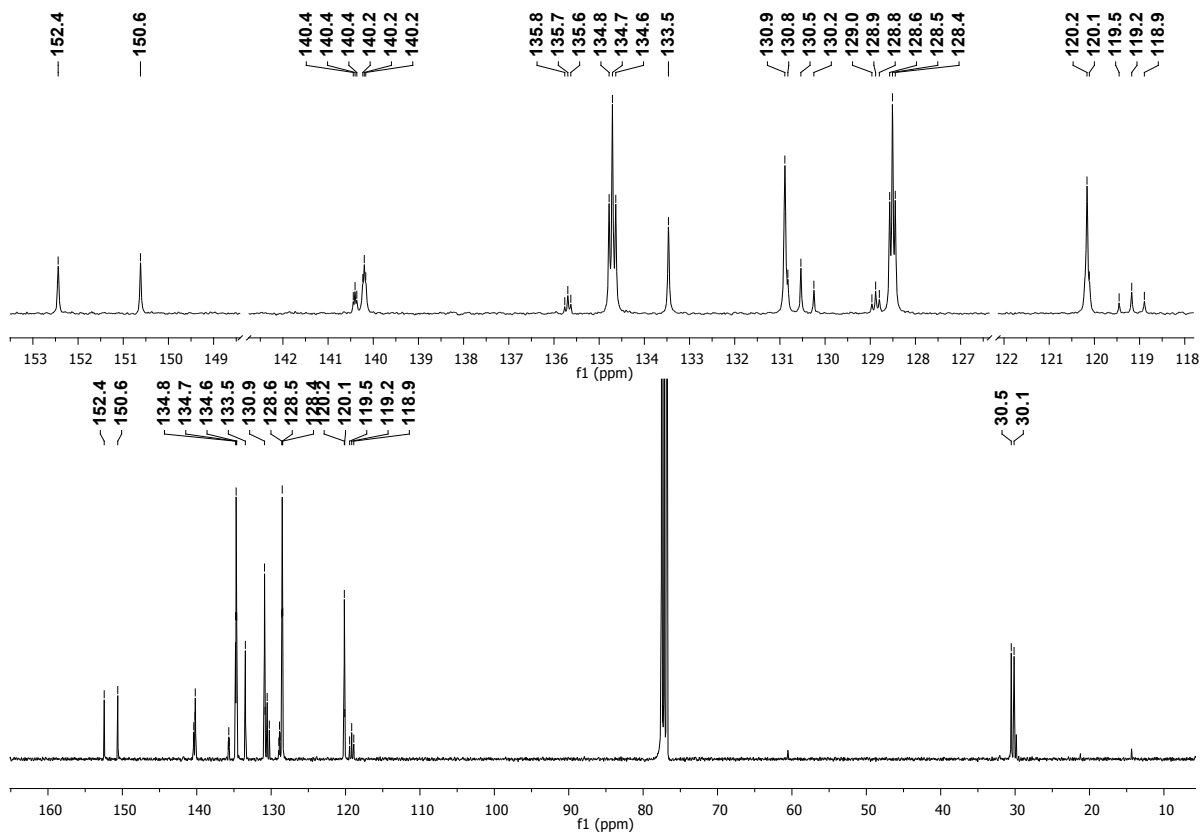


Figure S4b. $^{13}\text{C}\{^1\text{H}\}$ -NMR spectrum (CDCl_3) of 4.

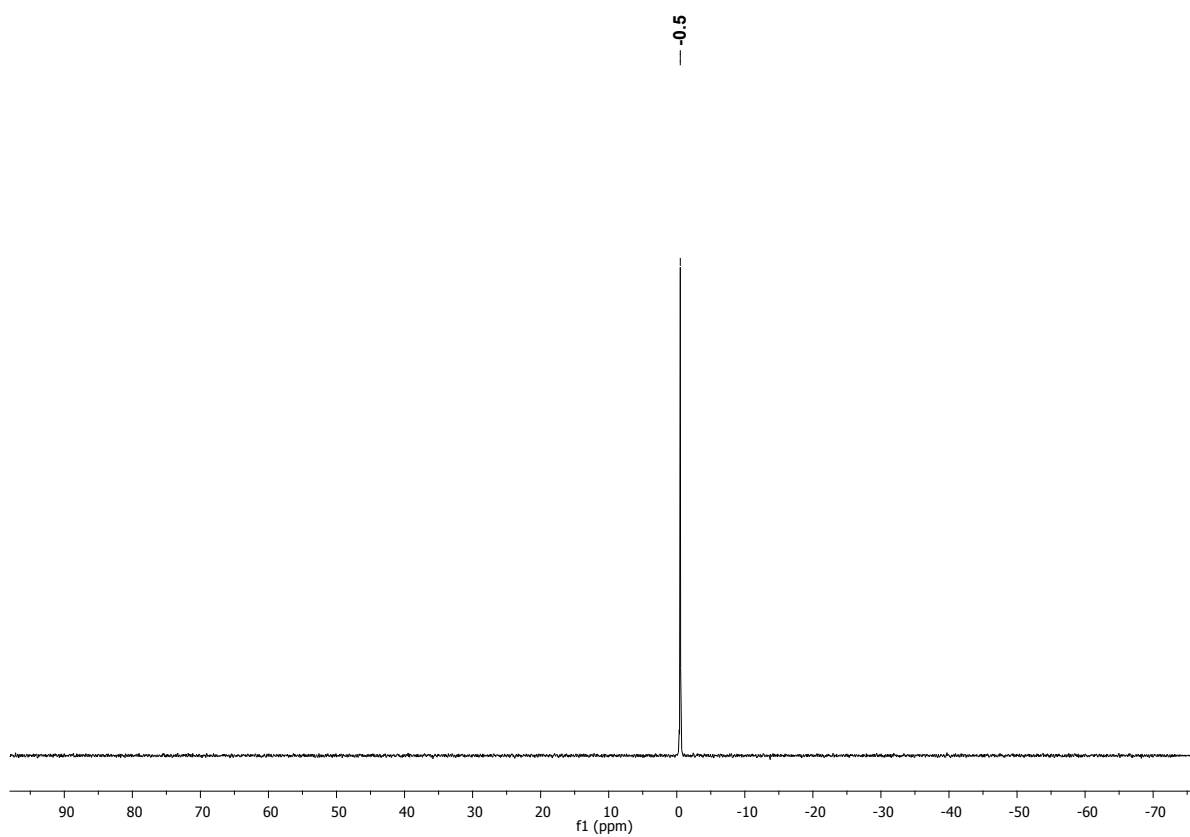


Figure S4c. $^{31}\text{P}\{^1\text{H}\}$ -NMR spectrum (CDCl_3) of 4.

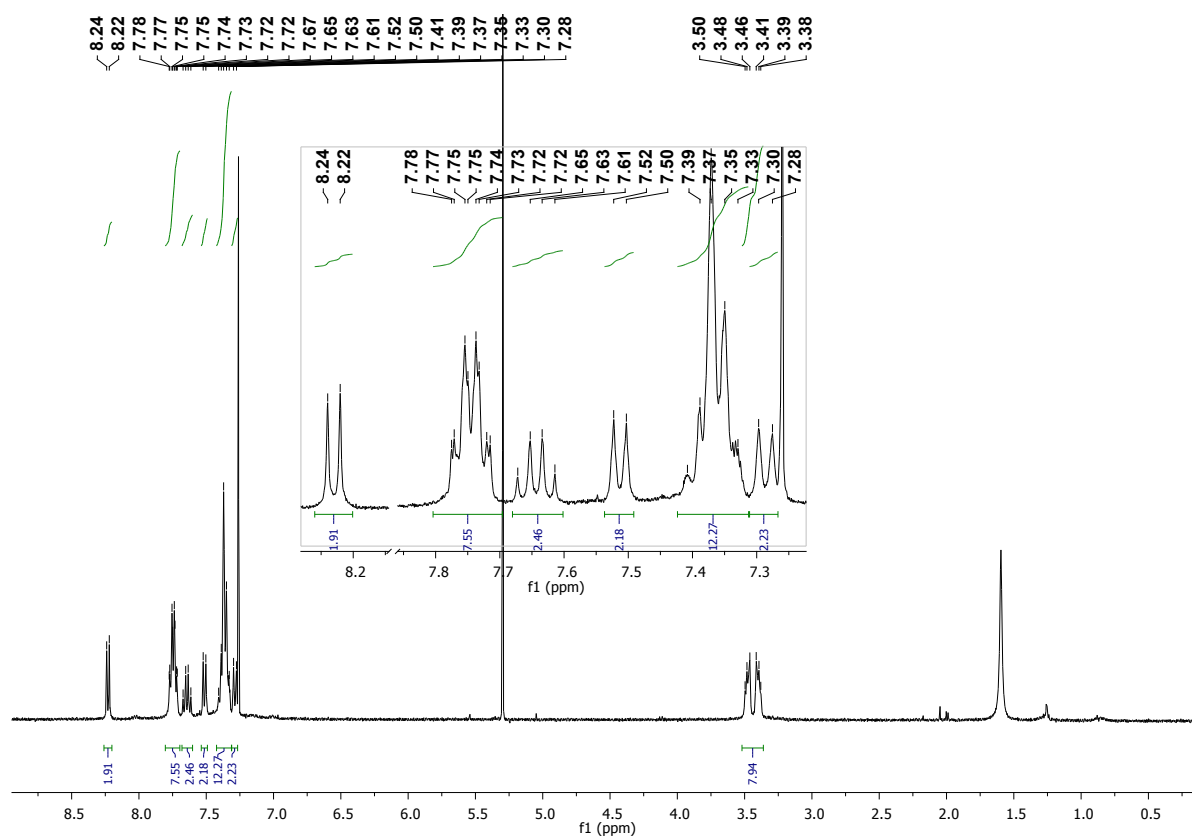


Figure S5a. ^1H -NMR spectrum (CDCl_3) of **5**.

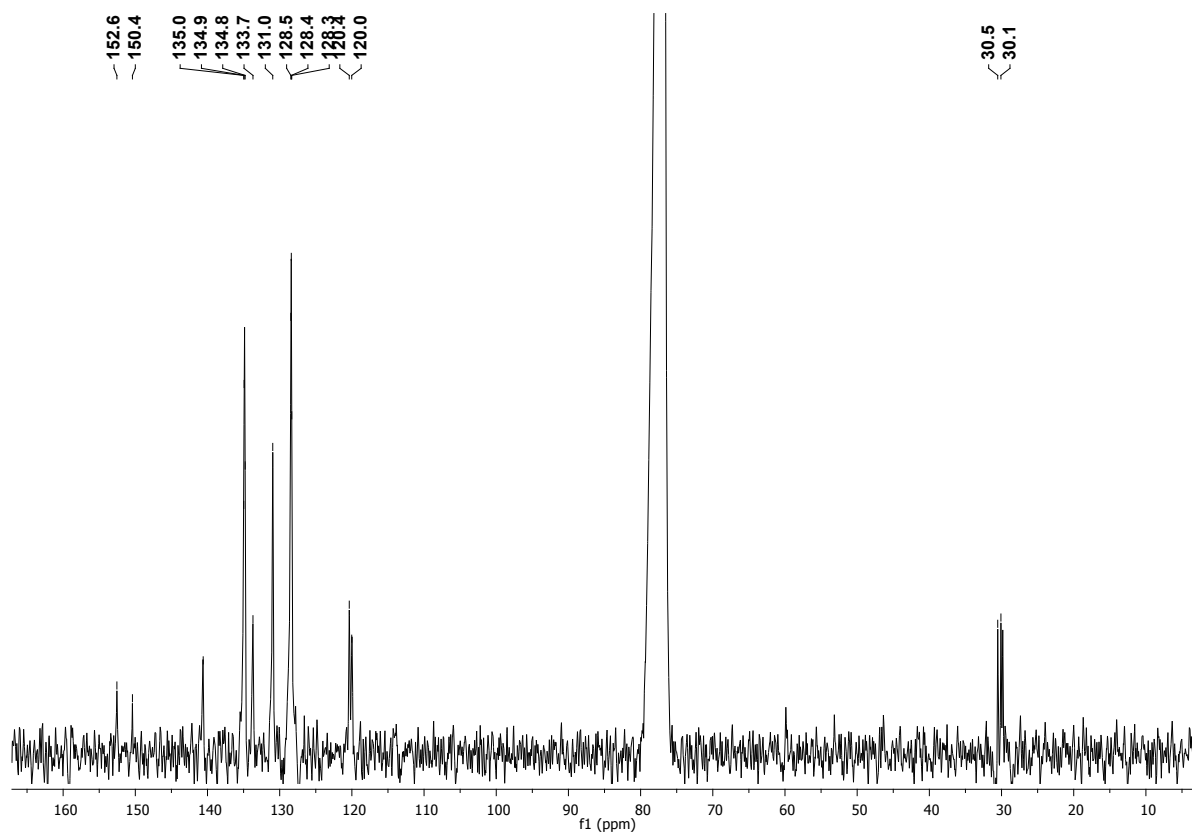


Figure S5b. $^{13}\text{C}\{^1\text{H}\}$ -NMR spectrum (CDCl_3) of **5** (poor solubility, acquisition time 72 h).

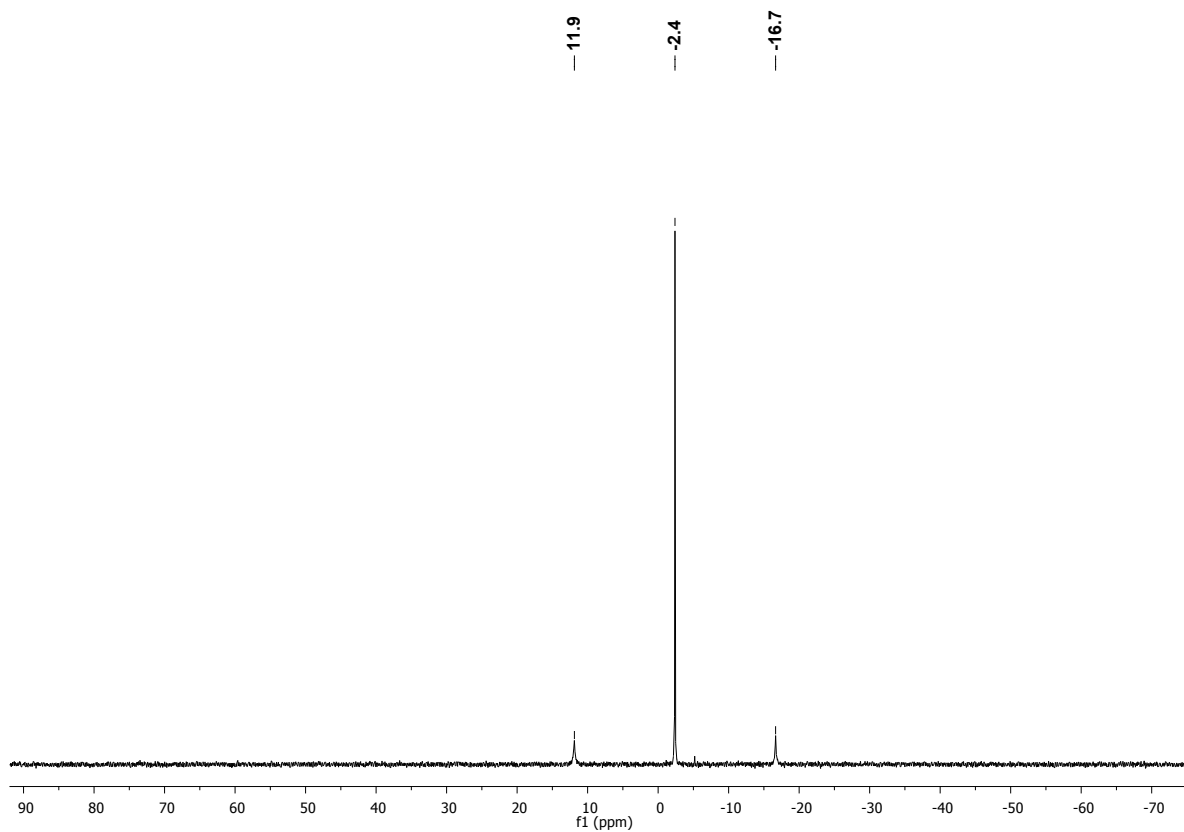


Figure S5c. ³¹P{¹H}-NMR spectrum (CDCl₃) of 5.

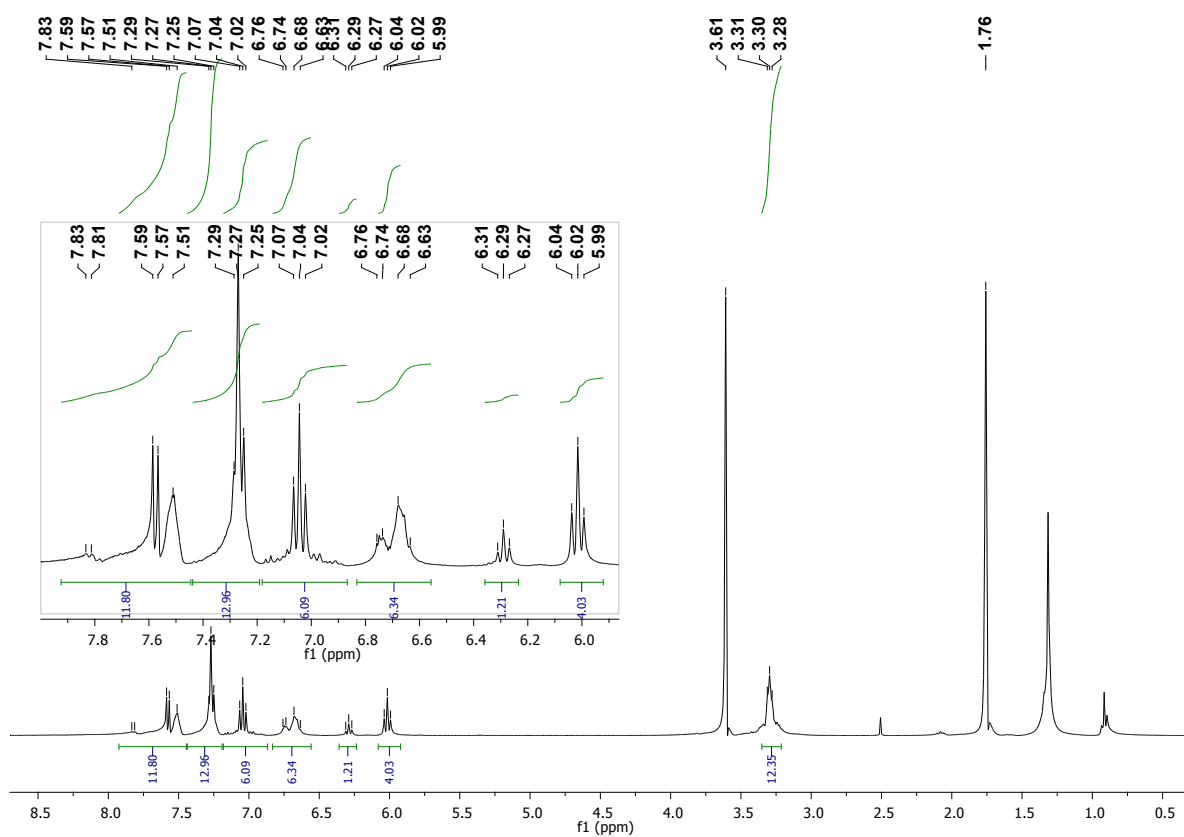


Figure S6a. ¹H-NMR spectrum (THF-d₈) of 6.

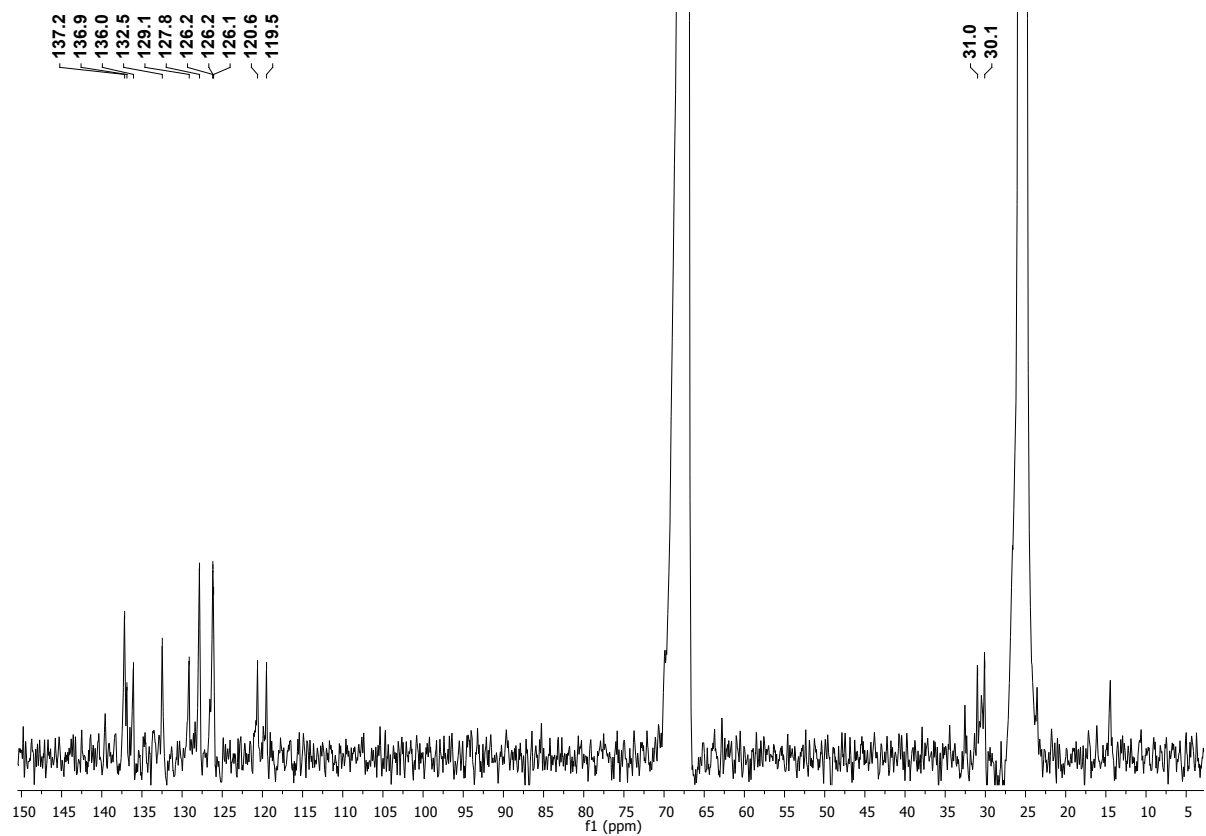


Figure S6b. $^{13}\text{C}\{^1\text{H}\}$ -NMR spectrum (THF- d_8) of **6** (poor solubility, acquisition time 24 h, decomposition in CDCl_3 and CD_2Cl_2).

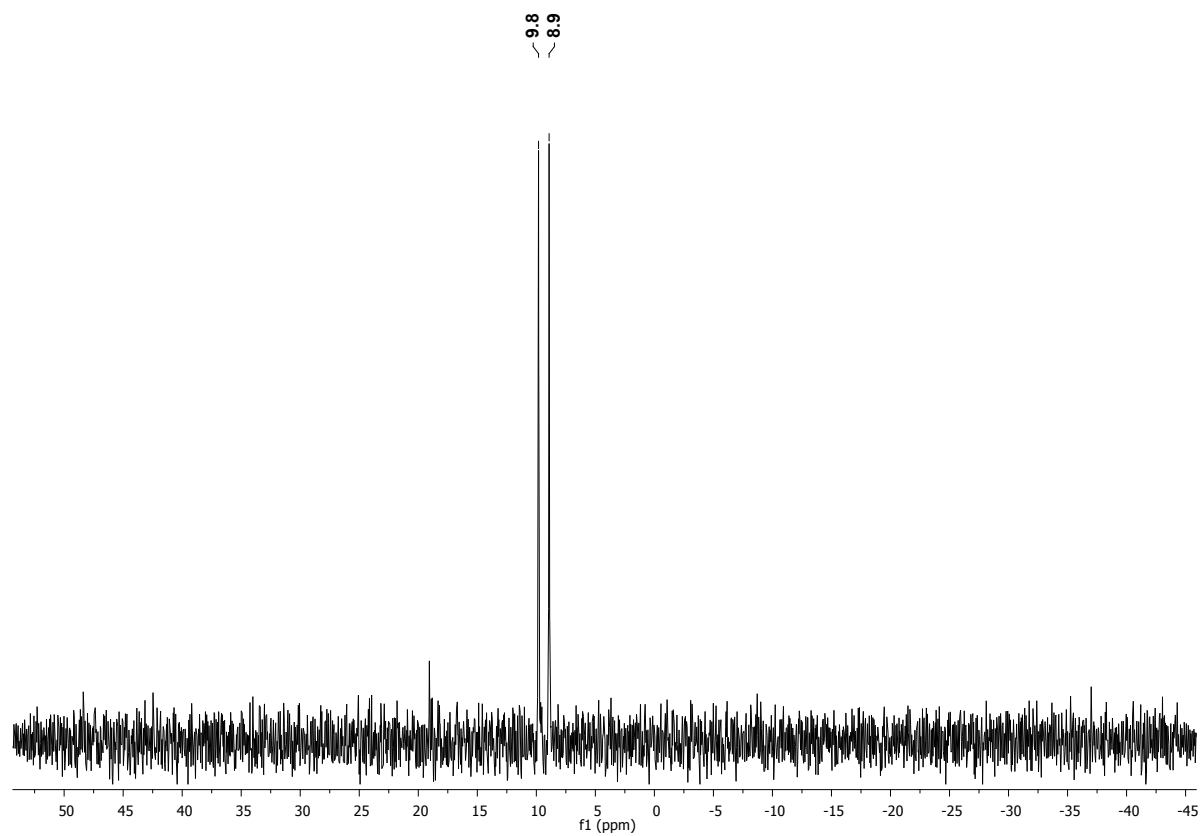


Figure S6c. $^{31}\text{P}\{^1\text{H}\}$ -NMR spectrum (THF- d_8) of **6**.

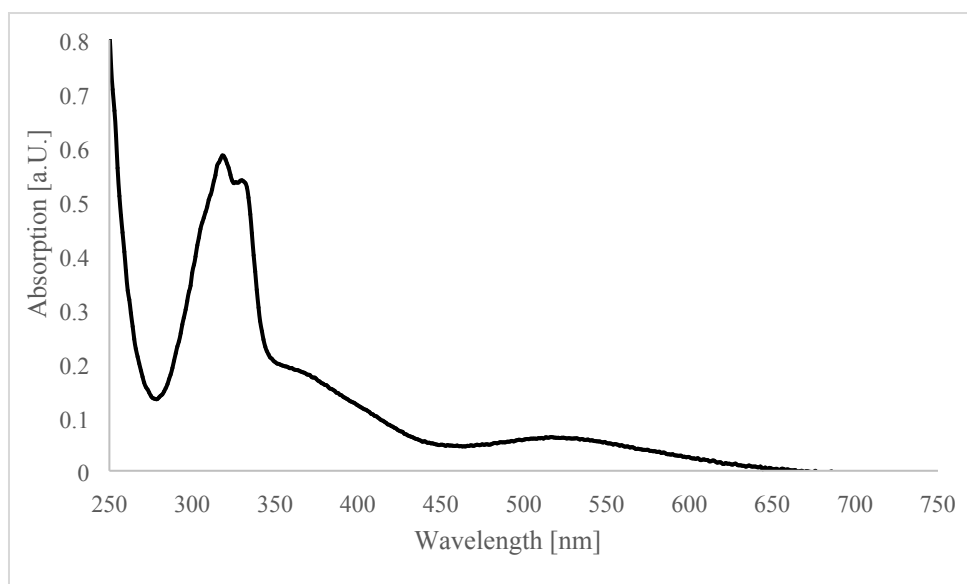


Figure S6d. UV/Vis spectrum (THF) of **6**.

Table S1. Selected interatomic distances (Å) and angles (°) of **1** and **2**.

	1	2
Bond Lengths and Angles		
Sb(1)–C(10)	2.187(2)	2.201(2)
Sb(1)–Cl(1)/C(70)	2.632(1)	2.192(2)
Sb(1)–C(40)	2.181(2)	2.203(3)
C(10)–Sb(1)–C(40)	93.14(9)	96.4(2)
C(10)–Sb(1)–Cl(1)/C(70)	91.68(7)	92.6(2)
C(40)–Sb(1)–Cl(1)/C(70)	92.28(7)	94.8(4)
peri Region Distances		
Sb(1)–P(1)	2.774(1)	3.171(1)
Sb(1)–P(2)	3.266(1)	3.229(1)
Sb(1)–P(3)		3.243(1)
peri Region Bond Angles		
Sb(1)–C(10)–C(19)	121.7(2)	125.3(3)
Sb(1)–C(40)–C(49)	126.8(2)	126.7(2)
Sb(1)–C(70)–C(79)		124.3(3)
C(10)–C(19)–C(18)	126.9(3)	129.1(3)
C(40)–C(49)–C(48)	129.4(2)	129.1(3)
C(70)–C(79)–C(78)		128.9(2)
P(1)–C(18)–C(19)	115.1(2)	120.9(2)
P(1)–C(48)–C(49)	117.8(2)	121.1(3)
P(1)–C(78)–C(79)		120.5(3)
Σ of bay angles	363.7(7)	375.3(7)
	374.0(6)	376.9(8)
		373.7(8)
Splay angle ^a	3.7(7)	15.3(7)
	14(6)	16.9(8)
		13.7(8)
Out-of-Plane Displacement		
P(1)	0.271(1)	0.016(1)
P(2)	0.510(1)	0.014(1)
P(3)		0.287(1)
Sb(1)	0.242(1)	0.019(1)
	0.462(1)	0.040(1)
		0.652(1)
Central Acenaphthyl Ring Torsion Angles		
C: (13)–(14)–(19)–(18)	178.9(3)	178.6(3)
C: (43)–(44)–(49)–(48)	–173.6(2)	–179.9(4)
C: (73)–(74)–(79)–(78)		173.4(3)
C: (15)–(14)–(19)–(10)	178.1(3)	–177.6(3)
C: (45)–(44)–(49)–(40)	–175.6(3)	–175.4(3)
C: (75)–(74)–(79)–(70)		176.3(5)

^a Splay angle: sum of the three bay region angles – 360.

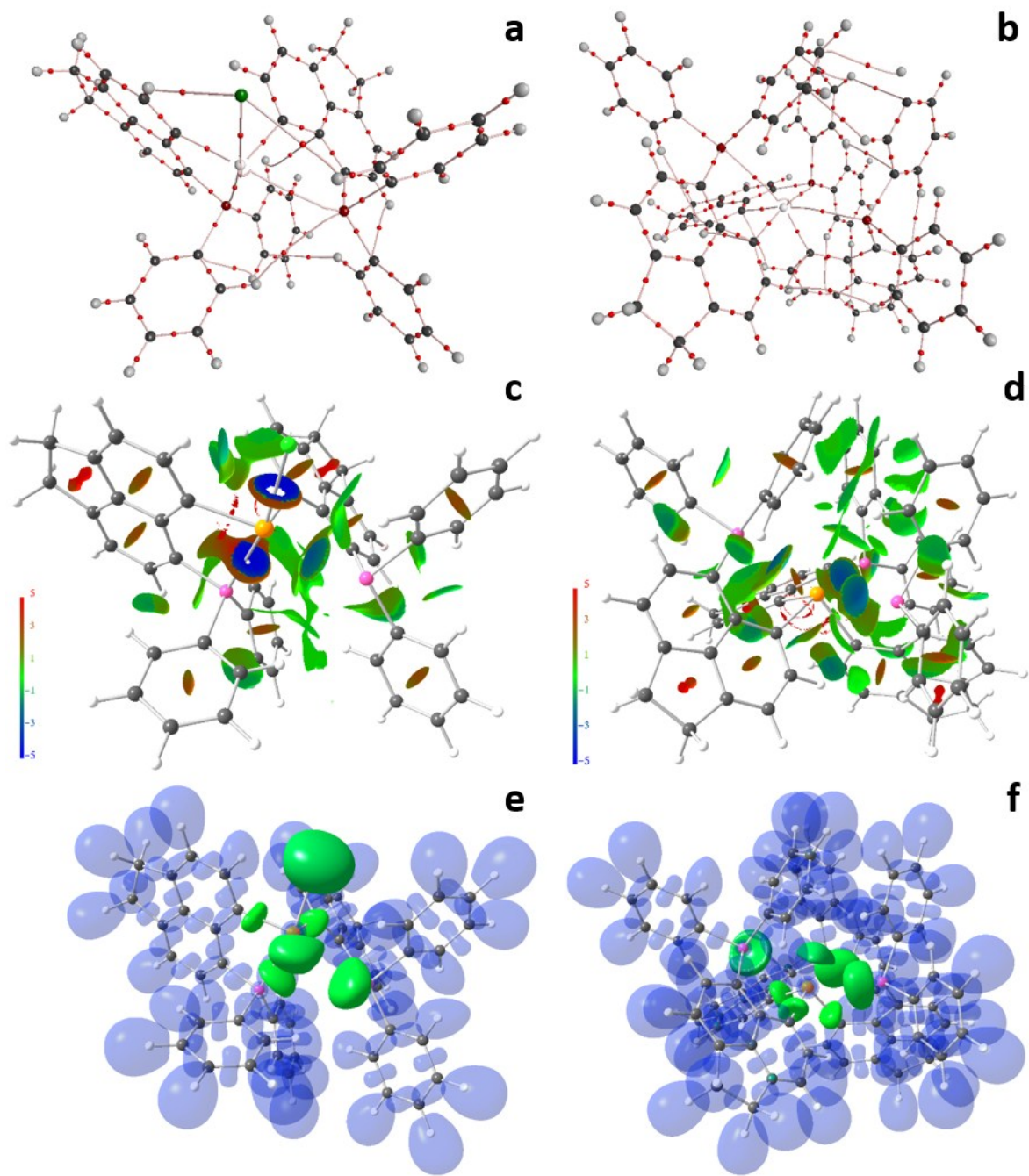


Figure S7. AIM topologies, NCI *iso*-surfaces ($s = 0.5$), and ELI-D *iso*-surfaces ($\gamma = 1.3$) of **1** (left column) and **2** (right column).

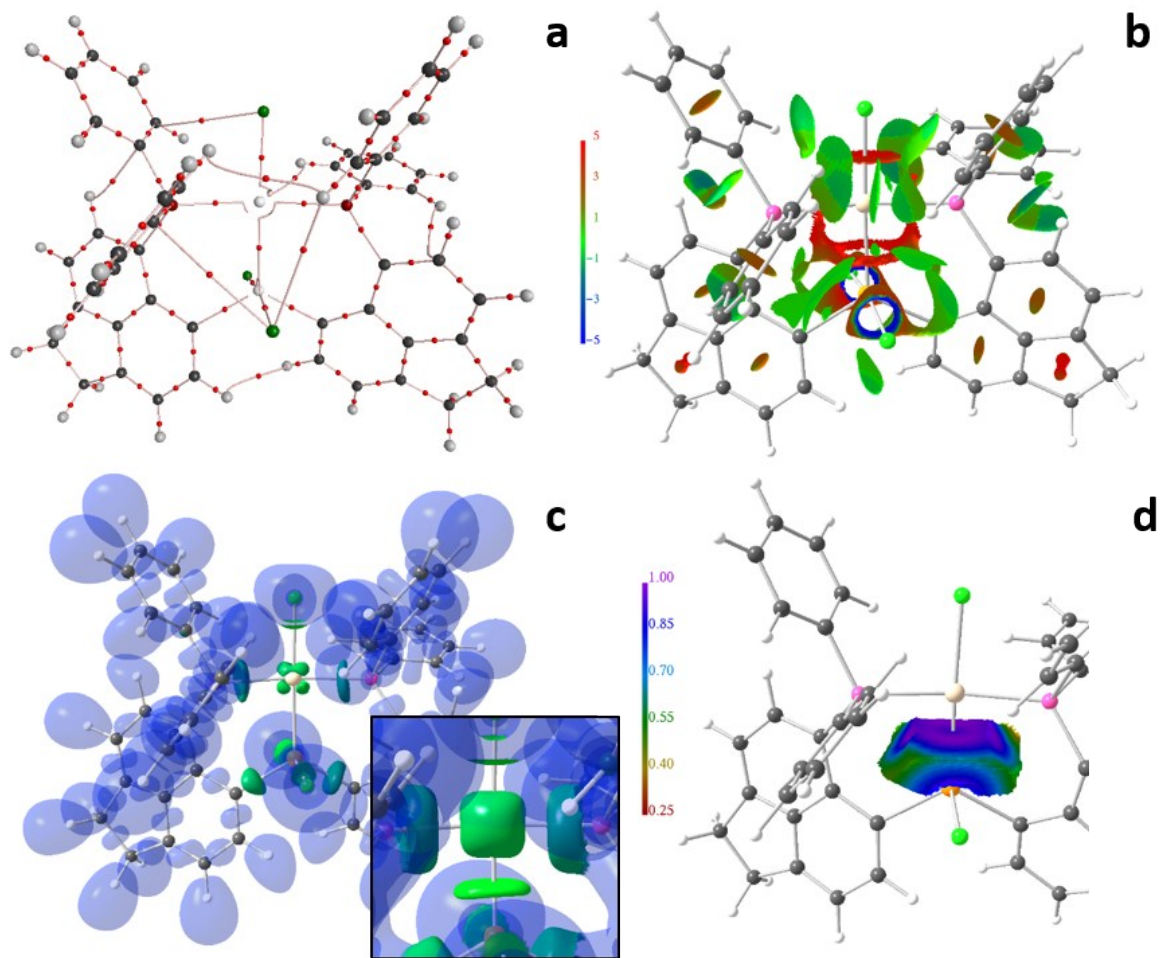


Figure S8. AIM topology, NCI *iso*-surface ($s = 0.5$), ELI-D *iso*-surface ($\gamma = 1.3$; inset shows magnification around the metal center at $\gamma = 1.25$), and ELI-D distribution mapped on the Sb-Pt ELI-D basin in **5**.

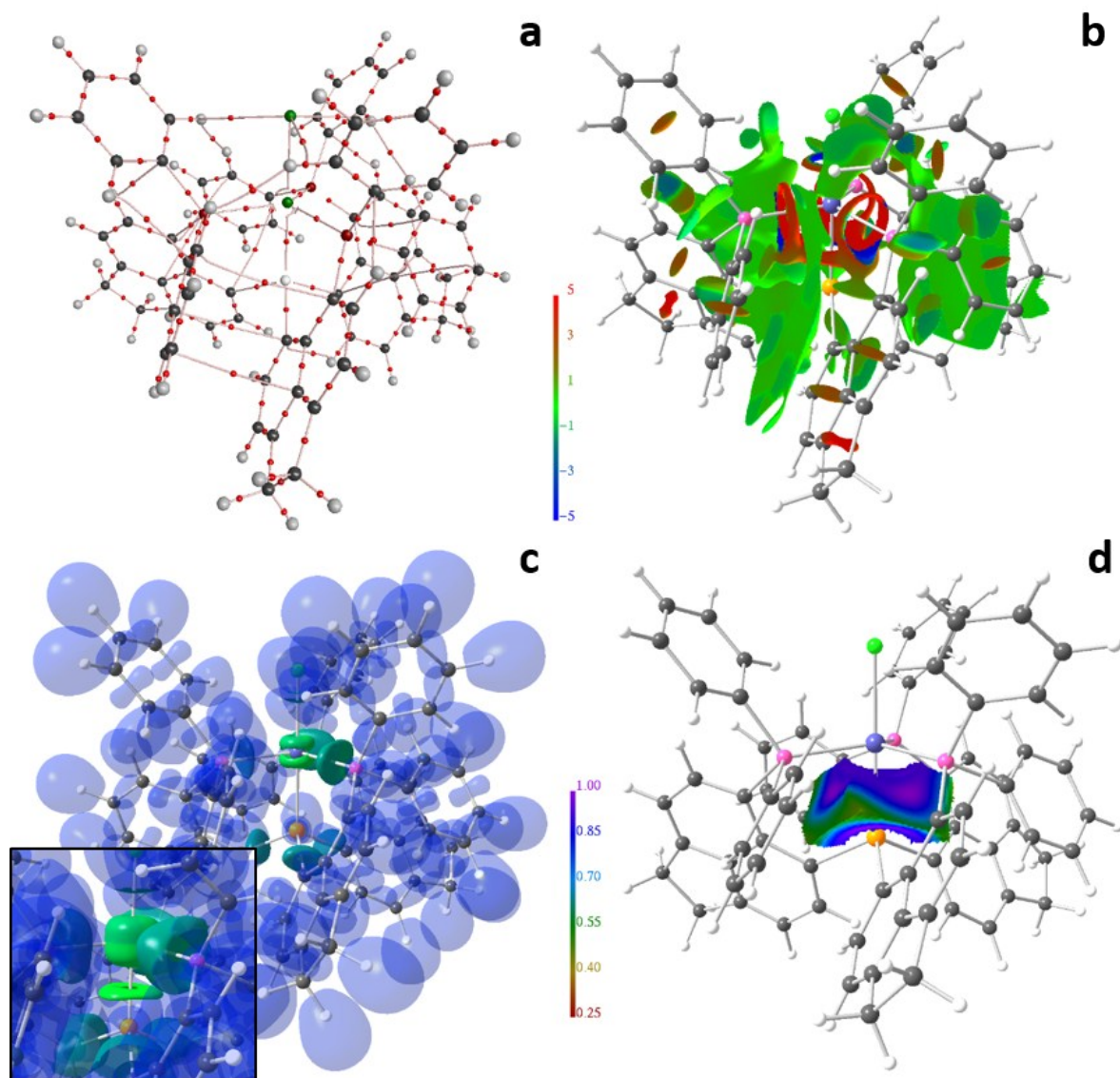


Figure S9 AIM topology, NCI *iso*-surface ($s = 0.5$), ELI-D *iso*-surface ($\gamma = 1.3$; inset shows magnification around the metal center at $\gamma = 1.25$), and ELI-D distribution mapped on the Sb–Rh ELI-D basin in **6**.